

Bradyrhizobium diazoefficiens cultures display phenotypic heterogeneity

Sukhvir K. Sarao¹, Armaan K. Sandhu¹, Ryan L. Hanson¹, Tanvi Govil², Volker S. Brözel^{1,3,*}

¹Department of Biology and Microbiology, South Dakota State University, 1224 Medary Avenue, Brookings, SD 57007, United States

²Karen M. Swindler Department of Chemical and Biological Engineering, South Dakota Mines, 501 E St Joseph Street, Rapid City, SD 57701, United States

³Department of Biochemistry, Genetics and Microbiology, Forestry and Agricultural Biotechnology Institute, University of Pretoria, Lunnon Road, Pretoria 0004, South Africa

*Corresponding author. Department of Biology and Microbiology, South Dakota State University, 1224 Medary Avenue, Brookings, SD 57007, USA.

E-mail: Volker.brozel@sdsu.edu

Abstract

Bacteria growing in liquid culture are assumed to be homogenous in phenotype. Characterization of individual cells shows that some clonal cultures contain more than one phenotype. Bacteria appear to employ bet hedging where various phenotypes help the species survive in diverse niches in soil and rhizosphere environments. We asked whether the agriculturally significant bacterium *Bradyrhizobium diazoefficiens* USDA 110, which fixes nitrogen with soybean plants, displays phenotypic heterogeneity when grown under laboratory conditions. We observed differential binding of sugar-specific lectins in isogenic populations, revealing differential surface properties. We employed Percoll™ density gradient centrifugation to separate clonal populations of exponential and stationary phase *B. diazoefficiens* into four fractions and characterized their phenotype by proteomics. Specific phenotypes were then characterized in detail. Fractions varied by cell size, polyhydroxyalkanoate content, lectin binding profile, growth rate, cellular adenosine triphosphate, chemotaxis, and respiration activity. Phenotypes were not heritable because the specific buoyant densities of fractions equilibrated within 10 generations. We propose that heterogeneity helps slow growing *B. diazoefficiens* proliferate and maintain populations in the different environments in soil and the rhizosphere.

Keywords: *Bradyrhizobium diazoefficiens*; phenotypic heterogeneity; soybean; proteomics; bet-hedging; soil; density gradient centrifugation

Introduction

Bradyrhizobium is an important and widely distributed soil bacterium that forms symbiotic association with legumes such as soybean and fixes atmospheric nitrogen. *Bradyrhizobium* have been reported in large numbers in soils across the world even in locations without leguminous plants [1]. Even in soybean fields, the majority of *Bradyrhizobium* in soil are never exposed to soybean roots. For long term population success, *Bradyrhizobium* cannot rely on nodulation but must be able to grow and survive in bulk soil. We recently found a diversity of *Bradyrhizobium* species in bulk soil and soybean rhizosphere [2]. The crosstalk between the bacterium and host soybean is very specific, and these interactions determine that only specific *Bradyrhizobium* strains form nodules. The non-nodulating *Bradyrhizobium* must persist outside of nodules. We found *B. diazoefficiens*, *Bradyrhizobium elkanii*, and *B. japonicum* inside nodules, the rhizosphere and bulk soil [2]. This occurrence of nodulating species in bulk soil far away from soybean roots indicated that they maintain populations independent of roots. This population success of *Bradyrhizobium* in soils indicates that it can adapt to multiple environments including nodules, the rhizosphere, and bulk soil where nutrients may be limiting.

Bacterial cells growing in homogenous liquid culture are assumed to be identical. An increasing number of studies indicate

that bacterial cells do not behave the same, but display more than one set of phenotypes termed phenotypic heterogeneity [3]. Heterogeneity in populations can be regulated to smaller or larger degrees. Tightly regulated heterogeneity involves a phenotype that is present or absent, such as spore formation in *Bacillus* [4], and flagellum expression in virulent *Salmonella* [5]. Other examples entail a spectrum of outcomes such as the level of nitrogenase in cells of *Klebsiella oxytoca* [6]. In select cases a very small proportion of the population displays the heterogeneity, such as in *E. coli* where some cells of antibiotic sensitive populations are slow growing and resistant, and termed persister cells [7]. In most cases, the phenotype sub-populations are more evenly distributed. For instance, *Salmonella typhimurium* exhibits phenotypic heterogeneity in expression of the virulence locus type-III secretion system [8]. *Saccharomyces* populations display heterogeneity in resistance to heat killing [9], and also in tolerance to lead [10]. *E. coli* displays heterogeneity in expression of genes involved in transition to stationary phase [11]. In addition, both exponential and stationary phase populations displayed a range in buoyant densities as determined by Percoll™ density gradient centrifugation. Fractions from the gradient displayed different levels of expression of stationary phase transition genes. Similarly, *Saccharomyces cerevisiae* displays heterogeneity in buoyant densities [12].

Received: 29 January 2025. **Revised:** 11 March 2025. **Accepted:** 24 March 2025

© The Author(s) 2025. Published by Oxford University Press on behalf of the International Society for Microbial Ecology.

This is an Open Access article distributed under the terms of the Creative Commons Attribution License (<https://creativecommons.org/licenses/by/4.0/>), which permits unrestricted reuse, distribution, and reproduction in any medium, provided the original work is properly cited.

Diversification of phenotypes benefits species occurring in heterogeneous environments. The different phenotypes in a population may be responsible for bet hedging or division of labor [13]. Heterogeneous expression of type III secretion system in *S. typhimurium* comes at a fitness cost to cells that engage host epithelial cells, benefitting other cells that do not express the system, an effective division of labor [8]. Taxa growing in heterogeneous or changing environments are better positioned for long term success through bet-hedging. A slow growing soil bacterium such as *Bradyrhizobium* cannot respond quickly to local changes and must have ways to adapt to these conditions and maintain populations until the next cropping season. Thus bet-hedging prepares species for survival under more than one possible set of conditions [14, 15].

We recently observed surface sugar differences in clonal liquid cultures as the fluorescently labeled lectins soybean agglutinin (SBA) and Wheat Germ Agglutinin (WGA) bound differentially [16, 17]. Some cells bound only to SBA, some to WGA, others to both, and many did not bind to either of the lectins, indicating at least four different surface phenotypes present. Members of *Rhizobiaceae* are very specific in their association with lectins produced by plants [18]. This indicated population heterogeneity for nodulation readiness where only some cells had lectin binding domains, while the remainder needed to rely on other traits to survive. We hypothesized that *B. diazoefficiens* USDA 110 displays phenotypic heterogeneity other than surface sugars. We targeted various stages in batch liquid culture, performed density gradient centrifugation using Percoll™, and characterized phenotypes of the fractions obtained. We found that isogenic populations were heterogeneous in various phenotypes including buoyant density, cell size, growth rate, polyhydroxyalkanoate (PHA) content, chemotactic ability, and cellular energetics.

Materials and methods

Cultures and culture conditions

B. diazoefficiens USDA 110 was obtained from the Culture Collection of the Agricultural Research Service, United States Department of Agriculture. USDA 110 was tagged with GFP as described recently [16]. *Bradyrhizobium diazoefficiens* spc 4 was obtained from Professor Hans-Martin Fischer (ETH, Zurich, Switzerland). *Bradyrhizobium diazoefficiens* USDA 110 and spc 4 were grown in PSY + arabinose as a carbon source [17]. For some experiments chloramphenicol was added to avoid contamination as USDA 110 is resistant to chloramphenicol.

The culture for inoculation was started from frozen glycerol stock, streaked for single colonies, one colony inoculated into liquid PSY with chloramphenicol, and maintained axenically. Cultures for all experiments were started by inoculating 500 μ l into 40 ml PSY media. Growth while shaking at 30°C was quantified for 120 h by O.D. (600 nm).

Density gradient centrifugation and staining of fractions

Samples for density gradient centrifugation were taken at early exponential, mid exponential, transition, and early stationary and late stationary phases (Fig. 1B). Cells were harvested by centrifugation at 7000 \times g for 7 min at 4°C and resuspended in 500 μ l sterile water. Percoll™ (Cat 17 089 101, Cytiva) was diluted with 0.15 M NaCl (final concentration of 240 mM) and gradients were prepared in polycarbonate centrifuge tubes (Cat 355 603, Beckman Coulter) by ultracentrifugation at 30000 \times g for 45 min (Beckman Optima Max MLA-55 rotor) at 4°C. Concentrated cell suspensions

were laid onto preformed gradients and centrifuged for one hour at 30000 \times g at 4°C. To determine respiratory activity, 10 ml liquid culture was pelleted at 7000 \times g for 7 min at 4°C and resuspended in 500 μ l of 0.01% triphenyl tetrazolium chloride (TTC) before layering onto gradients. Tubes were imaged using an iPhone 13 camera. Cell viability was determined by using LIVE/DEAD™ BacLight™ bacterial viability kit (Cat L13152, Invitrogen) to cell concentrates before centrifugation. Gradients were imaged using a stereo microscope with 466/440 nm excitation and a 525/550 nm emission filter. In all cases, gradients were separated into four fractions for all further experiments as defined in Fig. 1A. The fraction of lowest buoyant density (top fraction) was named fraction 1, and the highest buoyant density fraction was named fraction 4. Exponential phase fractions were named E1, E2, E3, and E4, and stationary phase were S1, S2, S3, and S4.

Lectin staining

To determine differential cell binding, lectin staining was performed on the individual fractions with fluorescein-conjugated SBA as described [17]. Samples were viewed by fluorescence microscopy using an Olympus BX53 Upright Compound Microscope with 466/440 nm excitation and a 525/550 nm emission filter and a 100- \times oil immersion objective, captured using an Olympus DP70 digital camera. Image J [19] was used to create composite images. To determine the effect of prior lectin binding on separation in the gradient, cells were pre stained with lectins before centrifugation.

Sample preparation for proteomics

Exponential phase density gradient fractions from four tubes were pooled into one tube. Percoll™ was removed from cells by filtering through polyvinylidene difluoride membranes with 0.2 μ m pore size (Cat HVLPO4700, Millipore). Percoll-free cells were obtained by cutting membranes into small pieces and transferring them into 15 ml conical tubes with 10 ml sterile water. Tubes were vortexed and shaken to dislodge cells from the membranes, filter pieces removed, and cells pelleted at 7000 \times g for 7 min at 4°C. Pelleted cells were resuspended in 450 μ l sample treatment buffer and placed on ice. Cells were disrupted by applying 2 bursts of 30 s each of ultra-sonication, placing on ice for 20 s between and after bursts. The unbroken cells were removed by centrifugation for 2 min at 12000 \times g. The supernatant was transferred to clean tubes and stored at -20°C. Protein was quantified using Coomassie Protein Assay Reagent (Cat 1 856 209, Thermo Scientific). The volume of sample required for a total of 1 μ g of protein was calculated and transferred to a 1 ml Eppendorf with 20 μ l DTT solution. Samples were resolved at 60 V for 30 min in Mini-PROTEAN TGX precast gels (Cat 4 561 094, BIO-RAD). Gels were stained using the Invitrogen Colloidal Blue Staining kit (Cat LC6025, Invitrogen), stained portions were excised and submitted to the Mass Spectrometry Facility at Carnegie Science, Stanford, CA.

Extracellular polymeric substances extraction and quantification

Percoll-free fractions of *B. diazoefficiens* USDA 110 were prepared as for proteomics. Cells were resuspended in 2 ml of 0.9% NaCl and 1 ml of 4 M NaOH, shaken for 1 h at 28°C, sonicated twice for 3 min and centrifuged at 5000 g for 15 min. The supernatant was supplemented with TCA to a final concentration of 7%, incubated at 4°C for 16 h, and centrifuged at 10000 \times g for 45 min at 4°C. Three volumes of absolute ethanol were added, incubated for 16 h at 4°C, and centrifuged at 4°C for 45 min. Residual liquid was removed by vacuum centrifugation and the extracellular polymeric

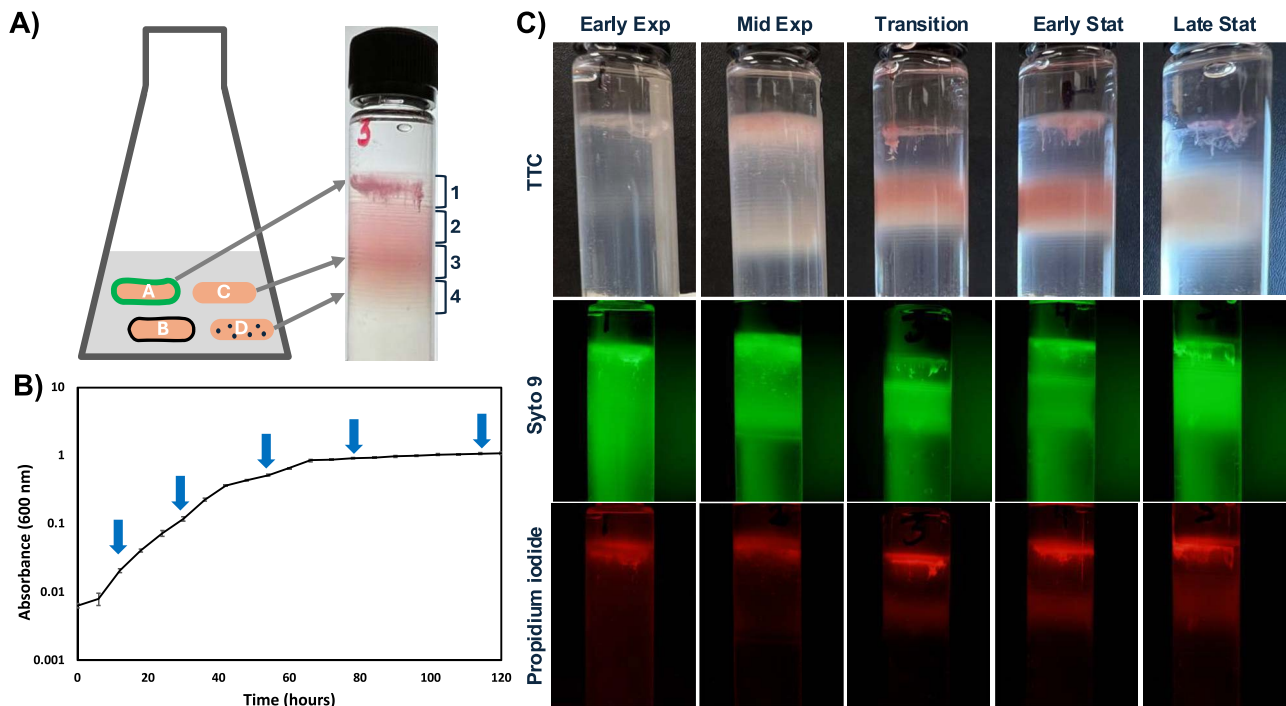


Figure 1. Separation of *B. diazoefficiens* USDA 110 subpopulations by Percoll™ density gradient centrifugation. We hypothesized that different phenotypes could be separated by their buoyant densities (A). Sampling time points for early exponential, mid exponential, transition, and early and late stationary phases were determined from the growth curve as indicated by arrows (B). Samples were subjected to density gradient centrifugation after staining with TTC or Syto 9 and propidium iodide (C). Images are representative of experiments performed on four occasions.

substances (EPS) pellets was suspended in 1 ml sterile water. Three aliquots of 30 μ l were mixed with 83 μ l of anthrone reagent (0.01 g anthrone, 0.5 ml ethyl acetate, and 5 ml concentrated H₂SO₄), incubated at 100°C for 4 min, and incubated on ice for 10 min. Absorbance was measured at 620 nm, and glucose equivalent derived using the standard curve.

Cell size determination

Exponential and stationary phase Percoll-free fractions of *B. diazoefficiens* USDA 110 (GFP) were prepared as for proteomics. Cells were harvested at 7000 \times g for 7 min at 4°C and resuspended in 3 ml sterile water. Drops of cell suspension were put on glass slides, covered with coverslip and the sides sealed with clear nail paint. Cells were imaged using an Olympus FV1200 Scanning Confocal microscope at 60X (oil immersion) using the GFP filter. Cell lengths were measured using ImageJ software [19]. For this, all cells in three separate microscopic views were measured, with a minimum of 50 cells per fraction.

Growth rate

Exponential phase fractions were prepared as described above. Undiluted, and fractions diluted by a factor of 20, 40, and 80, and 50 μ l were added to 200 μ l of PSY media (+ Arabinose and chloramphenicol) in a 96 well plate ($n = 16$). Plates were incubated at 30°C in a FLUOstar Omega plate reader (BMG LABTECH), and the absorbance (600 nm) measured every 10 min for 1500 minutes. Data were imported into Microsoft Excel to plot growth curves, and the generation times derived.

Polyhydroxyalkanoate

To determine presence of PHA, Percoll-free GFP labeled cells were stained with Nile red (Cat 415 711 000 Thermo Scientific) at 0.1 g/L and incubated for 30 min at room temperature. Cells were viewed

using an Olympus FV1200 Scanning Confocal microscope using green and red filters with a 60 X oil immersion objective. To visualize intracellular granules, exponential cells were washed twice using PBS (pH 7.4), resuspended in 5 ml EMC (100 mM sodium cacodylate, 2% glutaraldehyde, and 2% paraformaldehyde) and viewed by transmission electron microscopy at the Electron Microscopy Core Facility, University of Missouri.

To verify presence of PHA, cells were harvested, washed, and lysed in chloroform to selectively dissolve PHA and degrade the non-PHA cell components. An equal volume (v/v) of chilled ethanol (100%) was added to precipitate the PHA, followed by centrifugation and drying. The yield of PHA per gram of cells was calculated using the following equation.

$$\text{PHA Yield} = \frac{\text{PHA weight (g)}}{\text{Cells dry weight (g)}}$$

Fourier-transform infrared spectroscopy (FTIR) was used to analyze the functional groups in the sample structure, in a spectrum of 400 to 4000 cm^{-1} in the Agilent 600 FTIR spectrophotometer (Agilent Technologies, Santa Clara, CA, USA).

Measuring cellular activities

Cellular adenosine triphosphate

Percoll-free cell fractions were diluted to the same O.D, 100ul transferred to 1 ml microcentrifuge tubes, and 2.5 μ l of 1.2 M ice cold perchloric acid was added, mixed by vortexing for 10 s and put on ice for 15 min. The tubes were centrifuged at 30 000 \times g for 7.5 min at 4°C and 250 μ l of 0.72 M KOH and 0.16 M KHCO₃ was added. Tubes were vortexed and centrifuged at 30 000 \times g for 10 min at 4°C. 100 μ l of supernatant was transferred to a polystyrene 96 well plate and 100 μ l of BacTiter- Glo Microbial Viability Assay reagent (Cat G8230, Promega) was added. The plate

was put on a shaker for 5 min in the dark. Samples were transferred to a 96 well white plate and luminescence was measured using a luminometer (BioTek Synergy2 Microplate reader).

Cell respiration

Exponential cells of *B. diazoefficiens* USDA 110 (10 ml) were pelleted for 7 min at $7000 \times g$. Pellets were resuspended in $500 \mu\text{l}$ 0.01% TTC and left for 45 min. After density gradient centrifugation, four fractions of TTC stained cells were obtained and filtered to remove Percoll™ as explained above. All fractions were set at the same O.D. for normalization, and 5 ml of each fraction was transferred into a 10 ml tube and centrifuged at $7000 \times g$ for 7 min at 4°C . The pellet was resuspended in 1 ml autoclaved Millipore water. N-butanol (1 ml) was added and vortexed for 30 s. The suspension was centrifuged at $7000 \times g$ for 8 min at 4°C . The O.D. of the uppermost layer was measured at 490 nm. Non-TTC stained populations were used as blank.

Chemotaxis

The chemotactic response of various fractions was determined using a capillary tube assay with raffinose as chemoattractant [17]. Experiments were performed using three technical replicates and repeated on three separate occasions. Cell counts in P/10 without raffinose were determined and used as blank.

Heritability of phenotypes

To determine whether phenotypes of fractions/subpopulations were maintained during cell division, the four fractions were inoculated into PSY + arabinose with chloramphenicol and incubated for 5 and 10 generations at 30°C , after which density gradients were performed again.

Data analysis

Data were processed using Microsoft Excel, and statistical analyses were performed using PAST 4.03 [20], and Matlab [21]. Violin plots were generated using Matlab [21].

Results

Populations comprise subpopulations of different buoyant densities

Prior work on lectin binding to *B. diazoefficiens* had revealed that only sub populations bound to a specific lectin (Fig. S1) [17], indicating surface heterogeneity among cells. In a search for approaches to separate heterogeneous populations by phenotype, we were inspired by separation of *E. coli* and *S. cerevisiae* phenotypes by buoyant density [11, 22]. Buoyant density gradient centrifugation of exponential phase *B. diazoefficiens* revealed many bands with a less defined top domain (Fig. 1C), even more bands than visible in *E. coli* [11]. To determine whether phenotypic heterogeneity extended into stationary phase, we performed a growth curve to define early exponential, mid exponential, transition, and early stationary and late stationary (Fig. 1B). All growth phases evaluated resolved into many subpopulations, although the distribution of bands differed. Due to the large number of tightly spaced bands, we decided to separate the gradient into four fractions for all further experiments. We termed the top fraction, fraction 1 and the lowest, fraction 4 as shown in Fig. 1A. Because fraction 1 had the lowest buoyant density, the terms “most buoyant” and “upper fraction” were used interchangeably.

To determine if populations resolved by physiological state, we stained the cultures with TTC and observed presence of color in the various fractions. All fractions appeared pink, indicating

respiratory activity. We then resolved cultures stained with BaClight (syto 9 and propidium iodide) to see whether there were any dead cells. To view green and red fluorescence we photographed the same tubes at same magnification. The red fluorescence in the upper less defined top domain pointed to dead cells. Intense green fluorescence at the same locations questioned whether these cells were dead, or associated with eDNA. Microscopy of this upper domain showed that cells were entangled in clusters similar to as reported in *P. aeruginosa* [23]. Upon loading fractions in agarose gel, no fluorescence was seen, indicating that *B. diazoefficiens* did not produce eDNA at any of the growth phases in the medium used (Fig. S2). Therefore, we concluded that the red fluorescence in the upper domain reflected dead cells. Thus, the upper domain contained both live and dead cells. These results showed that liquid cultures of *B. diazoefficiens* contain cells of multiple different buoyant densities, indicating different phenotypes.

Cells with different surface properties can be separated by their buoyant densities

To determine surface sugar differences of various buoyant fractions, we performed lectin binding assay using SBA. The highest proportion of lectin binding cells occurred in E1 and S1, with fewer in E2 and S2, and very few in E3, S3, E4, and S4 (Fig. 2A, Fig. S3). Most of the cells binding lectin formed clusters. In contrast, cells in the lower fractions did not form clusters. To see whether these clusters are formed during ultra-centrifugation, we performed lectin binding on unseparated cultures. Clusters were observed in these cultures (Fig. 2B, Fig. S3). We have never observed large clusters in non-lectin-stained *B. diazoefficiens* liquid cultures suggesting that clusters form after exposure to SBA. To test this hypothesis, we added SBA to populations before loading on the gradient. Prior exposure to SBA yielded more compact upper domain (Fig. 2C vs D), with the lectin localized to the upper domain (Fig. 2E). The same phenomenon was observed for stationary phase populations (Fig. 2F). This suggested that SBA has a multivalent nature, cross linking cells into clusters [24].

Proteomics shows that fractions differ in only a few phenotypes

To obtain an overview of phenotypic differences among subpopulations, we opted for proteomics rather than transcriptomics because bacteria with larger genomes tend to display more post-transcriptional regulation [25], and the *B. diazoefficiens* genome is 9.1 Mb [26]. We performed proteomic analysis on the four exponential phase fractions. A total of 4594 of the 8283 predicted proteins were detected in exponential phase of *B. diazoefficiens* USDA 110 grown in PSY with arabinose (Table S1). Only 10 proteins were found to be significantly differentially abundant in E1 and E4 as per LFQ analysis in Frag pipe (using a cut-off of 0.05 adj. P-value, $1 \log_2\text{FC}$) (Fig. 3A). Because the fractions did not differ much at the proteome level, we did not anticipate a large number of phenotypic differences. To identify potential phenotypic traits for further investigation, we chose proteins that had a ratio between E1 and E4 of either >2 or <0.5 . From this list we selected proteins associated with a detectable phenotype, excluding proteins such as transcriptional regulators, with selected proteins highlighted in the supplementary spreadsheet. As PHA has been reported to vary among cells of rhizobial populations [27], we also selected proteins associated with PHA (PHB depolymerase family esterase and Phasin) (Fig. 3H and I).

Proteins involved in polysaccharide synthesis included UDP-glucose 4 epimerase and Glucarate dehydratase (Fig. 3B and C).

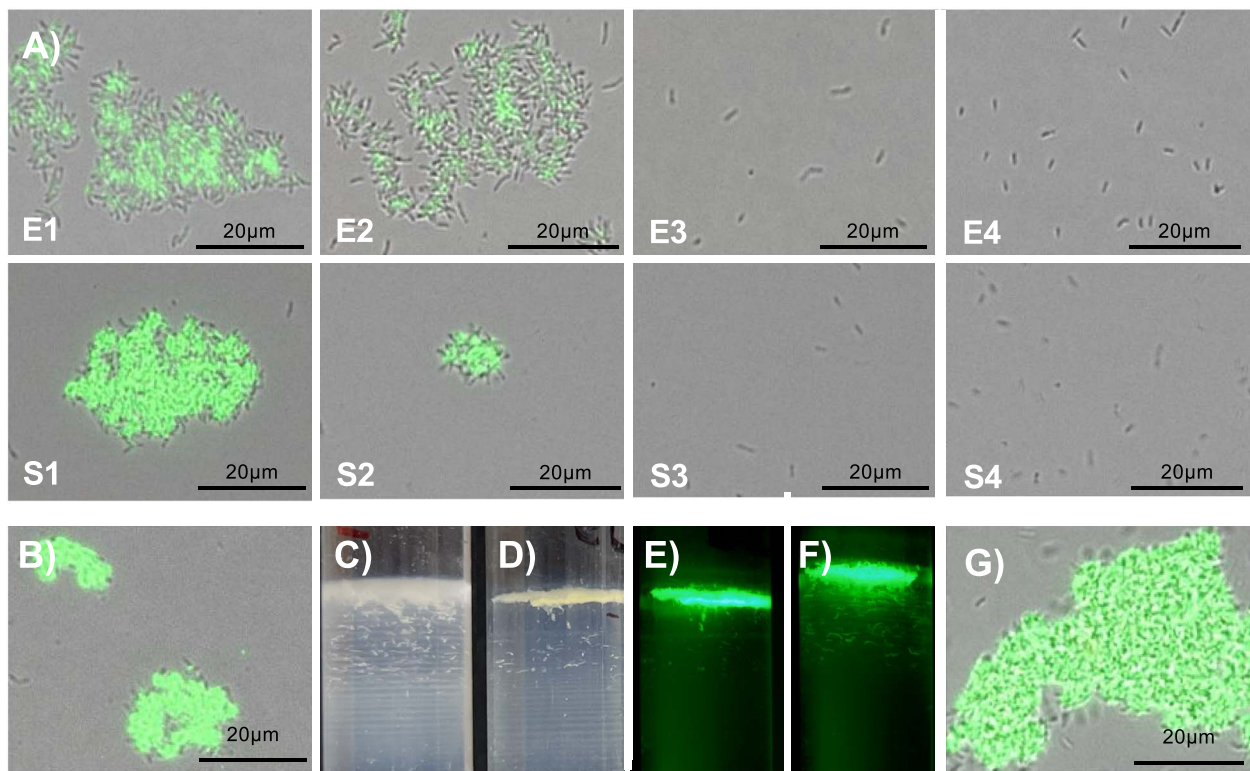


Figure 2. Lectin (SBA) binding profile of exponential and stationary phase fractions. Fractions exposed to fluorescein conjugated SBA (A) and unseparated exponential populations (B) were viewed by fluorescence microscopy. Gradients of exponential phase populations without (C) and with (D and E) prior treatment with SBA were viewed by illumination (C and D), and fluorescence (E). Stationary phase populations were pretreated with SBA and viewed by fluorescence (F), and fluorescence microscopy of the S1 showing association of cells by the lectin (G). Images are representative of experiments performed on three occasions.

Quantities of EPS in the four exponential phase fractions were near the detection limit (data not shown). EPS quantification of unseparated populations showed that EPS was produced from the transition phase onwards (Fig. S4). This is analogous to culturing on agar where young colonies are small and later become mucoid. Proteins involved in cell division (FtsZ), peptidoglycan synthesis (LysM peptidoglycan-binding domain) and membrane synthesis (Long-chain-acyl-CoA synthetase, and Flotillin) varied more than two-fold across the fractions (Fig. 3D–G). This prompted us to determine cell size and generation time of the four fractions (see next section). Proteins involved in chemotaxis (Chemotaxis protein and Methyl accepting chemotaxis protein) and motility (FliM Flagellar motor switch protein) (Fig. 3J–L) also varied across fractions. This prompted us to quantify chemotaxis of the four fractions.

Different buoyant density populations have different cell lengths and generation times

Cell sizes varied significantly amongst fractions of both exponential and stationary phase populations (Fig. 4A). The largest cells had the lowest buoyant density. This suggests that cell length is not proportional to density of cells. Interestingly, S1 contained much longer cells than E1. This is contrary to the established bacterial physiology based on *E. coli* where stationary phase cells are smaller than in exponential phase [28–30]. The observed differences in cell size prompted an investigation into generation times. Plotting of absorbance over time indicated that E4 cells grew faster (Fig. S5). Generation times of E4 (4.8 h), the smallest cells were significantly lower than E1 (5.45 h) and 2 (Fig. 4B). Again, this is contrary to the relationship between cell size and growth rate in *E. coli* [31]. Generation times of stationary phase

fractions were not determined because the population no longer increases.

Lowest density has highest proportion of cells with polyhydroxyalkanoate

Because PHA has been reported to vary among cells of rhizobial populations, we sought to quantify its distribution amongst cells of various fractions. Almost all the cells in E1 and S1 showed fluorescence with the lipophilic stain Nile Red. The lower fractions had significantly decreased proportions of cells with fluorescence (Fig. 5, Fig. S7). Stationary phase populations revealed higher proportions of fluorescence. The presence of PHA was confirmed by FTIR performed on extracts of exponential phase populations (Fig. 5J). TEM revealed multiple globules of low electron density (Fig. 5K and L). Intriguingly, red fluorescence was only viewed at one of the cell poles as were low electron density granules in TEM, whereas published images of PHA in *B. diazoefficiens* show granules distributed throughout cells [32, 33]. To determine whether polar localization was due to growth in liquid medium versus nodules, we inoculated soybean seedlings with two different strains i.e. *B. diazoefficiens* USDA 110 and *B. diazoefficiens* spc4. Bacteria extracted from the soybean nodules showed PHA granules distributed across the cells (Fig. S6). We did not explore this phenomenon further, but these results suggest that PHA localization may differ between liquid grown cells and bacteroids in nodules. Collectively, these results show that more PHA accumulated in E1 and S1 than the other fractions. The FTIR spectrum revealed several intense peaks, confirming its identity as PHA. The intense key peak at 1765 cm^{-1} indicated the presence of the ester carbonyl (C=O) stretching, [34], the predominant bond present in the backbone of PHAs.

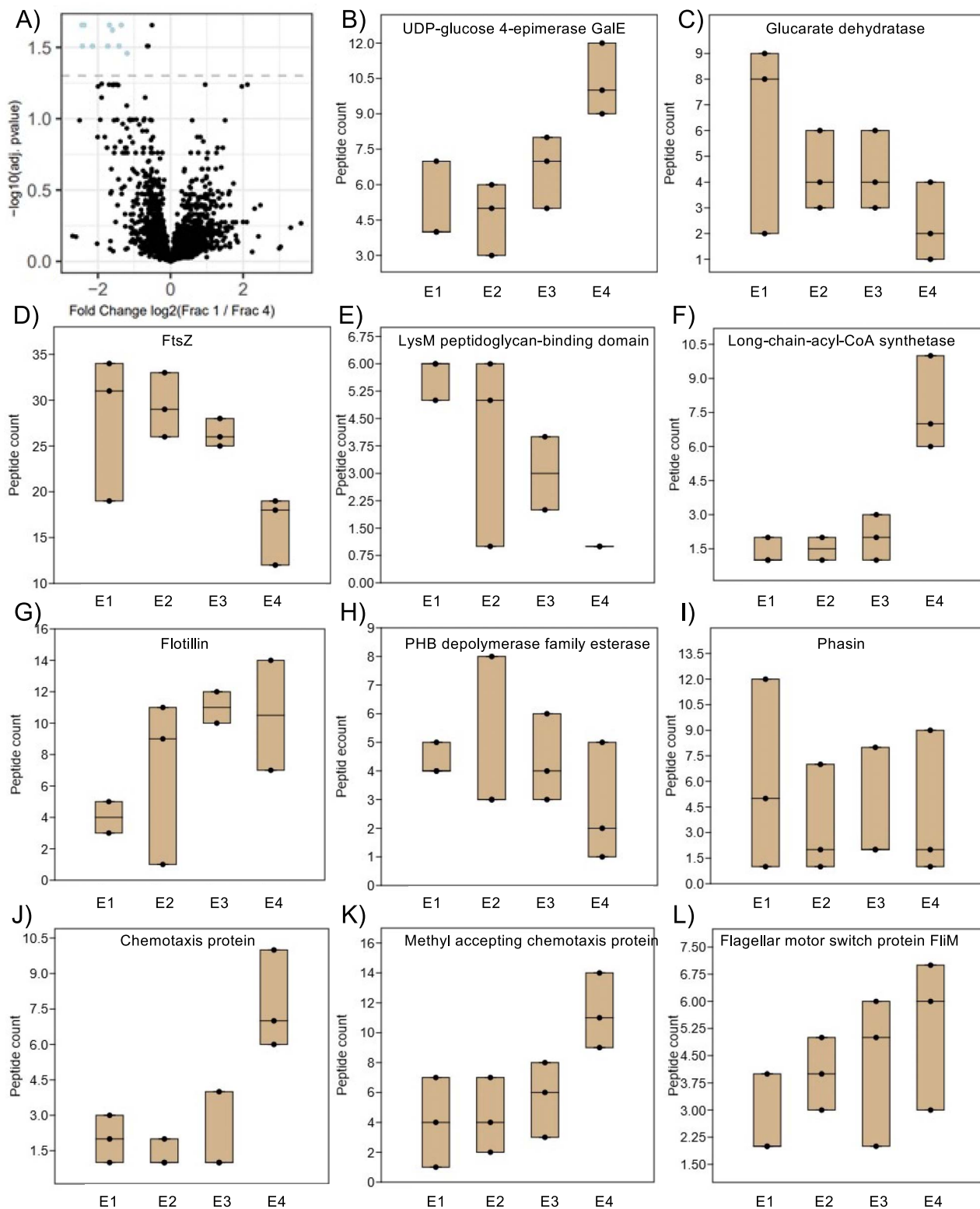


Figure 3. Proteomic characterization of the four exponential phase fractions by LC-MS. Volcano plot comparing E1 and E4, with significant differentially abundant proteins determined using a cut off of 0.05 of adjusted P value at \log_{10} (A). Representative proteins associated with EPS (B and C), cell envelope and division (D–G), PHA (H and I), and motility and chemotaxis (J–L) with greater than two fold or <0.5 are shown. The center lines indicate the median of data from three biological reps.

Different buoyant densities vary in cell activities and motility

To determine cell activity, TTC reduction and extracellular ATP per O.D. were quantified. E1 displayed higher respiratory activity (TTC

reduction) than the lower three fractions (Fig. 6A). Conversely, ATP levels per cell were lower in E1. This indicated that while E1 cells respired actively, they also consumed ATP generated more than the other fractions. To investigate the large number

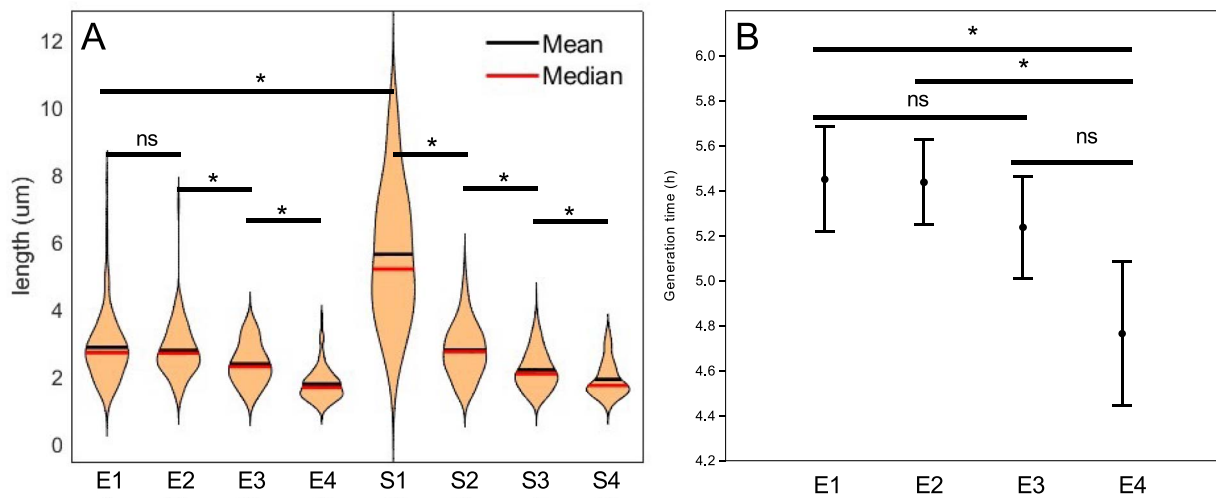


Figure 4. Cell sizes and growth rates of fractions. Exponential and stationary phase fractions differed (A), as did generation times of exponential phase fractions (B). The sizes of all cells in three separate microscopic views were determined, with a minimum of 50 cells. Growth rates were determined using 16 technical reps. The stars signify significant difference (Wilcoxon pairwise $P < .05$).

of chemotaxis related proteins in the lower fractions (Fig. 3), we quantified swimming toward the chemoattractant Raffinose. E3 populations showed the highest chemotaxis with E1 the lowest.

Phenotypes are not heritable

To determine whether fraction specific phenotypes were retained through multiple cell divisions, we cultured fractions for five and ten generations. Gradient centrifugation of fractions after five generations yielded bands that overlapped with the respective original fractions (Fig. 7). However, E1 included denser cells than the original fraction, indicating phenotypic changes in some of the cells. Likewise, fractions 3 and 4 also included zones with densities that differed to the original. Ten generations after separation into fractions, populations again included the full spectrum of buoyant densities. This indicated that fraction specific phenotypes were not retained during extended culturing, but that cells started diverging into multiple phenotypes again.

Discussion

B. diazoefficiens grows and maintain populations in soil and the rhizosphere, in addition to nodulating soybeans [2]. Competitive fitness in soil requires adaptability to different niches, so that bet-hedging through heterogeneous phenotypes would increase success of the species. We hypothesized that *B. diazoefficiens* displays phenotypic heterogeneity in phenotypes other than surface sugars. Density gradient centrifugation has previously been used to separate constituent phenotypes of an *E. coli* population, so we subjected various growth phase populations to Percoll™ density gradient centrifugation [11]. The density gradient yielded many tightly spaced bands, confirming differences in buoyant density, and therefore phenotypic heterogeneity of populations. Fractions obtained showed differential binding to SBA lectin, which confirmed our previous findings [17]. Proteomics revealed additional phenotypic differences among the fractions. Proteins associated with detectable phenotypes included polysaccharide synthesis, cell division, membrane and peptidoglycan synthesis, and chemotaxis, and we could confirm these differences in phenotypes among the various fractions. We also found differences in PHA content across fractions, as was reported for *Sinorhizobium meliloti* [27]. These results show that *B. diazoefficiens* displays phenotypic

heterogeneity in multiple phenotypes, and that each phenotype presents a spectrum.

Dichotomy v/s spectrum in heterogeneity

USDA 110 demonstrated a spectrum of heterogeneity in the various phenotypes tested. We observed a spectrum of cell sizes in the clonal population that separated into fractions (Fig. 4A). The top fraction of stationary phase included exceptionally longer cells, but the lengths of lower fractions varied less. Fraction 4 cells divided the fastest while fractions 3, 2, and 1 had similar growth rates. We did not see two phenotypes but a spectrum in regard to presence of PHA, as proportions of PHA positive cells decreased from fractions 1 to 4. Lectin binding also displayed a spectrum since most of the cells in E1 and S1 bound to lectins and formed clusters, with lesser binding in lower fractions. Cellular energetics, including ATP per cell and respiratory activity also showed a spectrum, as did motility (Fig. 8). Overall, all these phenotype spectrums indicate multiple sub populations. These spectra in phenotypes are in contrast to the established dichotomy in heterogeneity as first reported in 1976 for *lac* operon expression in *E. coli* [35]. Research in heterogeneity has focused on the presence or absence of a single phenotype in a homogenous population, viewing a phenotype dichotomously, as “A or B”. Examples of dichotomous heterogeneity include sporulation in *B. subtilis* where only some cells are primed to form endospores [36]. A second dichotomous phenotype in *B. subtilis* is competence [37]. A medically relevant example is flagellar expression in *Salmonella* [5]. *Salmonella* is also heterogeneous where some cells are virulent, whereas others take part in maintaining the population [38]. Dichotomous heterogeneity in phenotype has been interpreted as bet-hedging [39]. In contrast to dichotomous heterogeneity, some bacteria display a spectrum of heterogeneity. Nitrogenase in *K. oxytoca* is expressed heterogeneously, with individual cells having different levels of *nifHDK* mRNA as determined by RNA-FISH. This was ascribed to inherent stochasticity of transcription, likely through noise in the action of GlnK [6]. Another example of spectral heterogeneity is *Streptomyces* where colonies are developmentally heterogeneous, when within-colony phenotypic heterogeneity arises [40]. This allows part of the population to survive multiple shifts in conditions. Our results show that *B. diazoefficiens* displays heterogeneity on spectrums rather than dichotomously.

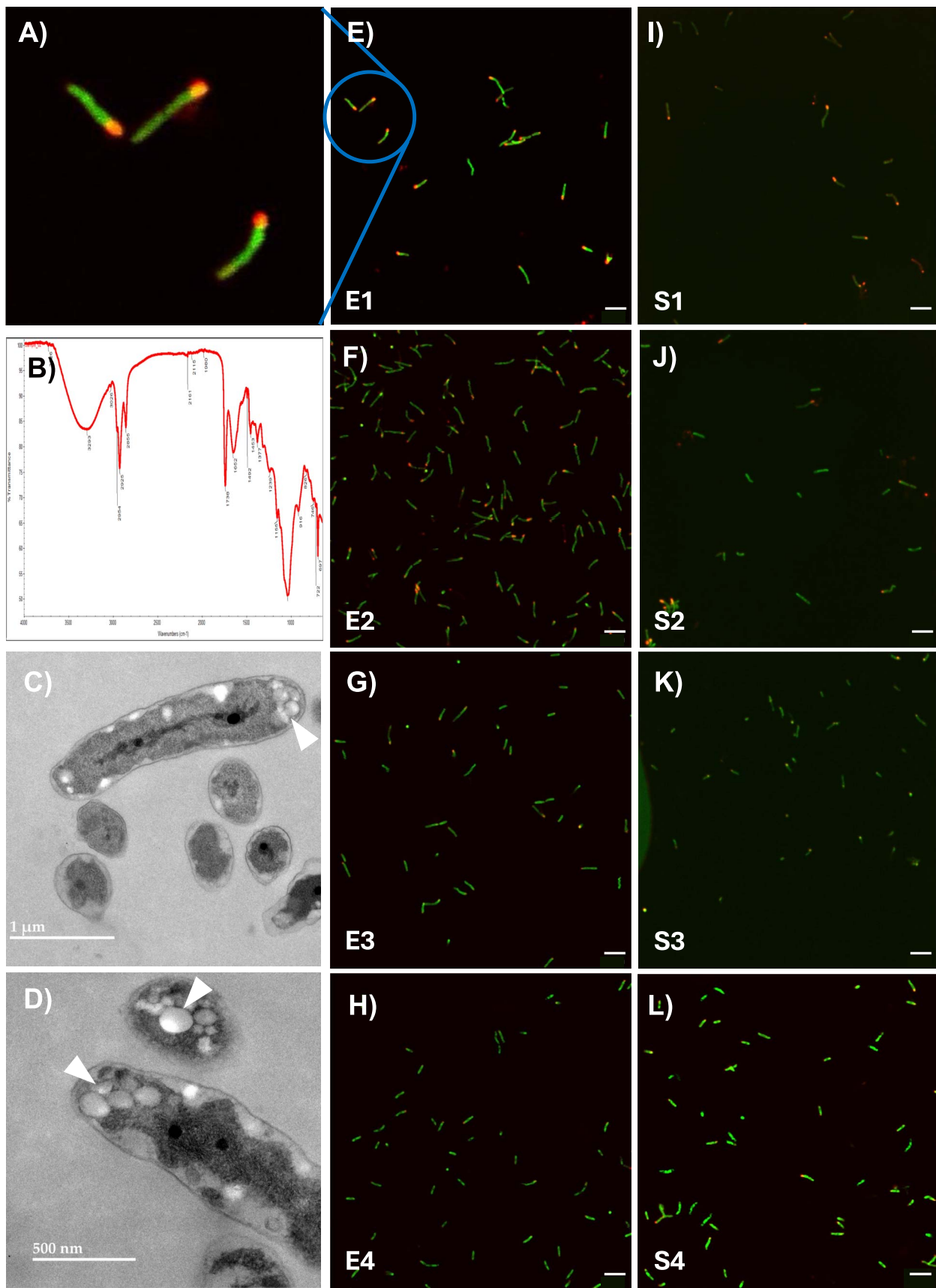


Figure 5. PHA distribution across fractions of exponential and stationary phase populations. PHA was visualized with Nile red and viewed by confocal microscopy (A–I). The presence of PHA was confirmed by the characteristic absorption bands of the extracted material by FTIR spectroscopy (J), and cellular distribution was visualized by scanning electron microscopy (K and L). Scale bars in e–l represent 5 μ m. Images for A and E–I are representative of experiments performed on three occasions, B on one occasion, and C–D on two occasions.

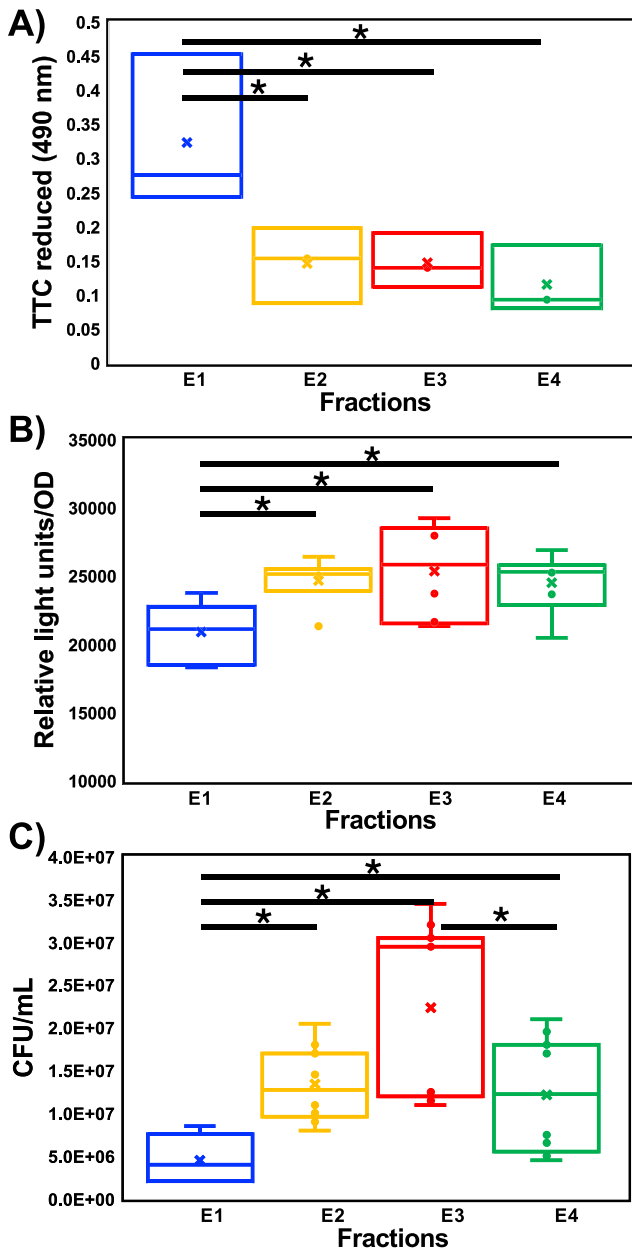


Figure 6. Respiratory activity was quantified by reduction of TTC (Tukey's pairwise, $P < .05$) (A) and ATP concentration (B) per CFU (Dunn's post-hoc, $P < .05$). Chemotaxis was compared by determining the CFU of populations attracted to Raffinose (C) (Dunn's post hoc, $P < .01$). TTC data (A) represents three biological reps with three technical reps each. ATP data (B) represents two biological reps with three technical reps each. Chemotaxis data (C) represent three biological reps with three technical reps each.

B. diazoefficiens USDA 110 displayed a range of intensities for each of multiple phenotypes (Fig. 8). This points to multiple subpopulations in culture growing under homogenous conditions. We propose that these ranges in multiple phenotypes position the culture for population success in the diverse conditions between bulk soil and soybean rhizosphere. While some cells should symbiotically associate with nodules, others are poised to persist in soils of varying nutrient and other properties. Thus, phenotypic heterogeneity would increase its survival under field conditions because of different input gradients, including concentration of nutrients in diverse environments like soil [40].

Cell size variation

B. diazoefficiens cells grown in PSY with arabinose were between 1 and 6 μm in length, in agreement with USDA 110 grown in YEM [41]. This differs from the paradigm for growth and cell division established in model bacteria such as *E. coli* and *B. subtilis* where cell length of daughter cells after division is identical. This is because peptidoglycan elongation synthesis in *E. coli* occurs across the cylindrical body of the rod, and septal synthesis occurs at midcell [42]. Thus, exponential phase cell lengths vary by a factor of two when grown under defined conditions. Recent work in Alphaproteobacteria indicates a different mechanism for cell elongation and division. The *Hyphomicrobiales* (*Agrobacterium tumefaciens*, *Brucella abortus*, and *S. meliloti*) display unipolar growth [43], as does *Caulobacter crescentus* [44]. Polar incorporation of envelope components relies on homologous proteins shared in the *Hyphomicrobiales*, and distinct from the canonical elongasome. Peptidoglycan incorporation in *B. diazoefficiens* was recently shown to occur unipolarly, like the other *Hyphomicrobiales* studied [41]. This unipolar growth is due to incorporation of new peptidoglycan only at one of the cell poles [45], leading to unidirectional growth from the new pole generated after cell division. Stationary phase USDA 110 included cells twice as long as in exponential phase, as seen in S1. This too differs from the *E. coli* paradigm where stationary phase cells are smaller than exponential phase [28]. These deviations from the model point to unique mechanisms of cell division and preparation for stationary phase. Collectively, these examples suggest that USDA 110 displays dimorphism, dividing asymmetrically, and yielding cells of varying sizes and phenotypes.

Heritability of phenotypes

Individual fractions cultured for ten generations reverted to the full range of buoyant densities, indicating that buoyant density was not heritable. Even after five generations the density range of individual fractions expanded. The phenotype of specific fractions was not maintained across ten cell divisions. This suggests that the phenotype was not controlled through epigenetic imprints on individual genomes [46]. Rather, phenotypic variation arose through cell division. Phenotypic heterogeneity can be due to regulatory mechanisms or to stochasticity where the outcome is random [47, 48]. Heterogeneity subject to regulatory mechanisms is termed bi- or multi-stability and should display repeatable behavior. The heterogeneous phenotypes observed from homogenous culture conditions appeared repeatedly. This included buoyant density distribution, PHA, lectin binding profile, chemotaxis, and cell activity. The repeatable appearance of these phenotypes points to underlying regulatory mechanisms rather than stochasticity in gene expression. Thus, the occurrence of multiple phenotypes under homogenous conditions in liquid medium indicates an established mechanism for heterogeneity in USDA 110. The species appears to have evolved to differentiate into different phenotypes during division.

Model

Growing *B. diazoefficiens* populations appear poised to divide into cells with different phenotypes. Various cells then have the capacity to occupy various niches depending on the functions they can perform. Phenotypic heterogeneity has been likened to bet-hedging where each cell type performs specific functions [39]. This is beneficial to species occurring in complex or changing environments such as soil where physicochemical conditions vary. Resident microbiota consume available carbon, and growing

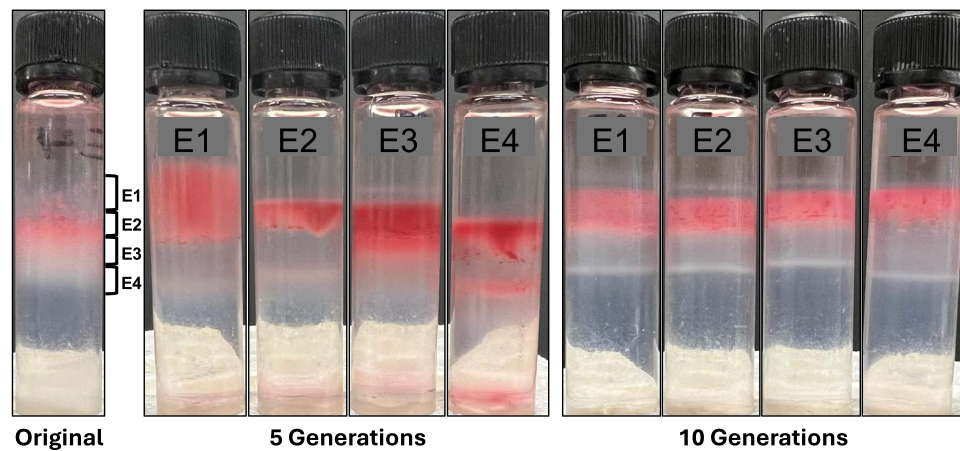


Figure 7. Heritability of phenotypes after 5 and 10 generations. Four fractions from the original exponential phase gradient were cultured for five and ten generations and subjected to Percoll density gradient centrifugation. Images are representative of experiments performed on two occasions.

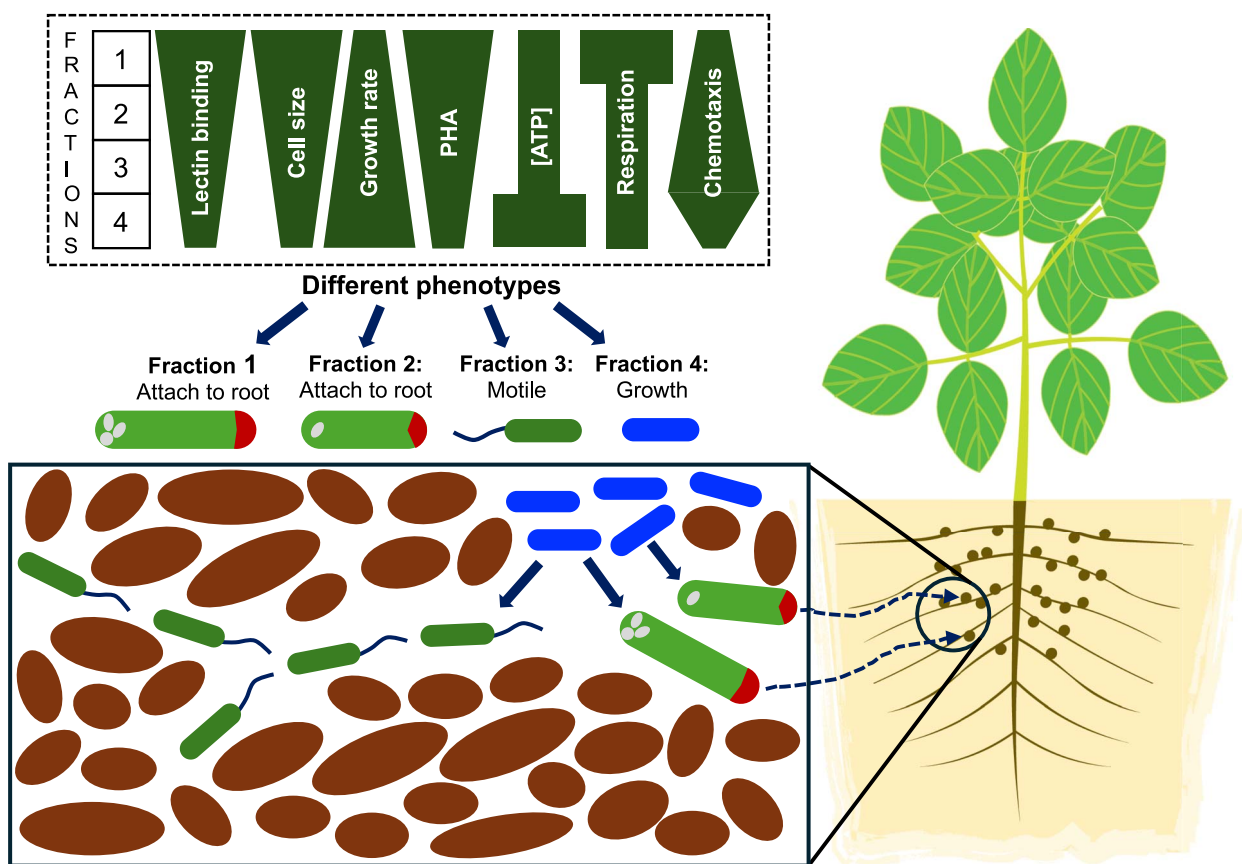


Figure 8. Proposed model for ecological fitness of *B. diazoefficiens* phenotypes. The box at the top shows differences in specific phenotypes across the four fractions. The phenotypes suggest that E1 cells are best prepared for nodulation, E3 cells for chemotaxis toward beneficial niches, and E4 cells for population growth in soil.

root systems such as soybean introduce increased complexity through localized exudation of organic molecules that may act as nutrients or signals to bacteria [49]. Depending on the locality vis-à-vis growing soybean roots, *Bradyrhizobium* encounter feast or famine. Roots provide organic carbon for growth and entry points for nodulation, but distal locations may lack growth-supporting carbon. The range of traits observed (Fig. 8) may each benefit species' success in some way. While some cells would symbiotically associate with nodules, others could be poised to persist

in soils of varying nutrient and other properties. This would ensure that part of the progeny would succeed, irrespective of the set of local conditions. Larger cells with lectin-binding domains and reserve carbon in form of PHA (E1) are best poised for root adherence and ensuing nodulation. Smaller motile cells (E3) can translocate better through pores in soil, supporting dispersal of the species. Small faster growing cells, while not prepared for nodulation, divide faster contributing to population expansion (E4).

Conclusion

Laboratory grown *Bradyrhizobium* comprised of sub populations with different phenotypes, which included cell size, PHA content, lectin binding profile, growth rate, cellular ATP, chemotaxis, and respiration activity. As these phenotypes play roles in population success in the heterogeneous soil and soybean rhizosphere environments, we propose that heterogeneity helps slow growing *B. diazoefficiens* proliferate and maintain populations.

Author contributions

SS and VB designed the study with inputs from AS. VB planned the experiments and supervised the project. SS performed experiments assisted by AS and TG. SS, AS, RH and VB analyzed the data. SS and VB wrote the manuscript with inputs from AS, TG, and RH. All authors provided critical feedback and helped to shape the manuscript.

Supplementary material

Supplementary material is available at ISME Communications online.

Conflicts of interest

The authors declare that they have no competing interests.

Funding

Sukhvir Kaur Sarao was supported by a National Science Foundation assistantship. This work was supported by the National Science Foundation/EPSCoR RII Track-1: Building on the 2020 Vision: Expanding Research, Education and Innovation in South Dakota, Award OIA-1849206 and by the South Dakota Board of Regents. This material is based upon work conducted using the South Dakota State University Functional Genomics Core Facility (RRID:SCR_023786) supported in part by the National Science Foundation/EPSCoR Grant No. 0091948, the South Dakota Agricultural Experiment Station, and by the State of South Dakota. Research, and by the National Institute of General Medical Sciences of the National Institutes of Health under Award Number P20GM135008. The content is solely the responsibility of the authors and does not necessarily represent the official views of the National Institutes of Health.

Data availability

Raw data sets are available from the corresponding author.

References

- Delgado-Baquerizo M, Oliverio AM, Brewer TE et al. A global atlas of the dominant bacteria found in soil. *Science* 2018;**359**:320–5. <https://doi.org/10.1126/science.aap9516>
- Sarao SK, Boothe V, Das BK et al. *Bradyrhizobium* and the soybean rhizosphere: species level bacterial population dynamics in established soybean fields, rhizosphere and nodules. *Plant Soil* 2024. <https://doi.org/10.1007/s11104-024-06814-4>
- Davis KM, Isberg RR. Defining heterogeneity within bacterial populations via single cell approaches. *BioEssays* 2016;**38**:782–90. <https://doi.org/10.1002/bies.201500121>
- Errington J. *Bacillus subtilis* sporulation: regulation of gene expression and control of morphogenesis. *Microbiol Rev* 1993;**57**:1–33.
- Stewart MK, Cummings LA, Johnson ML et al. Regulation of phenotypic heterogeneity permits salmonella evasion of the host caspase-1 inflammatory response. *Proc Natl Acad Sci* 2011;**108**:20742–7. <https://doi.org/10.1073/pnas.1108963108>
- Bashir T, Brackston RD, Waite C et al. Molecular origins of transcriptional heterogeneity in diazotrophic *Klebsiella oxytoca*. *Msystems* 2022;**7**:e00596–22. <https://doi.org/10.1128/msystems.00596-22>
- Keren I, Kaldalu N, Spoering A et al. Persister cells and tolerance to antimicrobials. *FEMS Microbiol Lett* 2004;**230**:13–8. [https://doi.org/10.1016/S0378-1097\(03\)00856-5](https://doi.org/10.1016/S0378-1097(03)00856-5)
- Westerman TL, Bogomolnaya L, Andrews-Polymeris HL et al. The *Salmonella* type-3 secretion system-1 and flagellar motility influence the neutrophil respiratory burst. *PLoS One* 2018;**13**:e0203698. <https://doi.org/10.1371/journal.pone.0203698>
- Levy SF, Ziv N, Siegal ML. Bet hedging in yeast by heterogeneous, age-correlated expression of a stress protectant. *PLoS Biol* 2012;**10**:e1001325. <https://doi.org/10.1371/journal.pbio.1001325>
- Holland SL, Reader T, Dyer PS et al. Phenotypic heterogeneity is a selected trait in natural yeast populations subject to environmental stress. *Environ Microbiol* 2014;**16**:1729–40. <https://doi.org/10.1111/1462-2920.12243>
- Makinoshima H, Nishimura A, Ishihama A. Fractionation of *Escherichia coli* cell populations at different stages during growth transition to stationary phase. *Mol Microbiol* 2002;**43**:269–79. <https://doi.org/10.1046/j.1365-2958.2002.02746.x>
- Rieder SE, Emr SD. Isolation of subcellular fractions from the yeast *Saccharomyces cerevisiae*. *Curr Protoc Cell Biol*. <https://doi.org/10.1002/0471143030.cb0308s08>
- Ackermann M. A functional perspective on phenotypic heterogeneity in microorganisms. *Nat Rev Microbiol* 2015;**13**:497–508. <https://doi.org/10.1038/nrmicro3491>
- Veening J-W, Smits WK, Kuipers OP. Bistability, epigenetics, and bet-hedging in bacteria. *Ann Rev Microbiol* 2008;**62**:193–210. <https://doi.org/10.1146/annurev.micro.62.081307.163002>
- Grimbergen AJ, Siebring J, Solopova A et al. Microbial bet-hedging: the power of being different. *Curr Opin Microbiol* 2015;**25**:67–72. <https://doi.org/10.1016/j.mib.2015.04.008>
- Sandhu AK, Brown MR, Subramanian S et al. *Bradyrhizobium diazoefficiens* usda 110 displays plasticity in the attachment phenotype when grown in different soybean root exudate compounds. *Front Microbiol* 2023;**14**:1190396. <https://doi.org/10.3389/fmicb.2023.1190396>
- Sandhu AK, Subramanian S, Brözel VS. Surface properties and adherence of *Bradyrhizobium diazoefficiens* to glycine max roots are altered when grown in soil extracted nutrients. *Nitrogen* 2021;**2**:461–73. <https://doi.org/10.3390/nitrogen2040031>
- Hirsch AM. Role of lectins (and rhizobial exopolysaccharides) in legume nodulation. *Curr Opin Plant Biol* 1999;**2**:320–6. [https://doi.org/10.1016/S1369-5266\(99\)80056-9](https://doi.org/10.1016/S1369-5266(99)80056-9)
- Rasband WS. *ImageJ*. Bethesda, Maryland, USA: U. S. National Institutes of Health. <https://imagej.net/ij/>, 1997-2018.
- Hammer Ø, Harper DA. Past: paleontological statistics software package for education and data analysis. *Palaeontol Electron* 2001;**4**:1.
- Violin HH. M-simple violin plot using matlab default kernel density estimation. *INRES (University of Bonn), Katzenburgweg* 2015;**5**:53115.
- Vanoni M, Vai M, Popolo L et al. Structural heterogeneity in populations of the budding yeast *Saccharomyces cerevisiae*.

- J Bacteriol* 1983;**156**:1282–91. <https://doi.org/10.1128/jb.156.3.1282-1291.1983>
23. Okshevsky M, Meyer RL. The role of extracellular DNA in the establishment, maintenance and perpetuation of bacterial biofilms. *Crit Rev Microbiol* 2015;**41**:341–52. <https://doi.org/10.3109/1040841X.2013.841639>
 24. Cecioni S, Imberty A, Vidal S. Glycomimetics versus multivalent glycoconjugates for the design of high affinity lectin ligands. *Chem Rev* 2015;**115**:525–61. <https://doi.org/10.1021/cr500303t>
 25. Miravet-Verde S, Lloréns-Rico V, Serrano L. Alternative transcriptional regulation in genome-reduced bacteria. *Curr Opin Microbiol* 2017;**39**:89–95. <https://doi.org/10.1016/j.mib.2017.10.022>
 26. Baraquet C, Dai W, Mendiola J et al. Transposon sequencing analysis of *Bradyrhizobium diazoefficiens* 110 spc4. *Sci Rep* 2021;**11**:13211. <https://doi.org/10.1038/s41598-021-92534-z>
 27. Ratcliff WC, Kadam SV, Denison RF. Poly-3-hydroxybutyrate (phb) supports survival and reproduction in starving rhizobia. *FEMS Microbiol Ecol* 2008;**65**:391–9. <https://doi.org/10.1111/j.1574-6941.2008.00544.x>
 28. Akerlund T, Nordström K, Bernander R. Analysis of cell size and DNA content in exponentially growing and stationary-phase batch cultures of *Escherichia coli*. *J Bacteriol* 1995;**177**:6791–7.
 29. Roszak D, Colwell R. Survival strategies of bacteria in the natural environment. *Microbiol Rev* 1987;**51**:365–79.
 30. Kolter R, Siegel DA, Tormo A. The stationary phase of the bacterial life cycle. *Ann Rev Microbiol* 1993;**47**:855–74.
 31. Trueba FJ. On the precision and accuracy achieved by *Escherichia coli* cells at fission about their middle. *Arch Microbiol* 1982;**131**:55–9. <https://doi.org/10.1007/BF00451499>
 32. Quelas JI, Mesa S, Mongiardini EJ et al. Regulation of polyhydroxybutyrate synthesis in the soil bacterium *Bradyrhizobium diazoefficiens*. *Appl Environ Microbiol* 2016;**82**:4299–308. <https://doi.org/10.1128/AEM.00757-16>
 33. Quelas JI, Mongiardini EJ, Pérez-Giménez J et al. Analysis of two polyhydroxyalkanoate synthases in *Bradyrhizobium japonicum* usda 110. *J Bacteriol* 2013;**195**:3145–55. <https://doi.org/10.1128/JB.02203-12>
 34. Awasthi S, Srivastava P, Singh P et al. Biodegradation of thermally treated high-density polyethylene (hdpe) by *Klebsiella pneumoniae* ch001. *3 Biotech* 2017;**7**:332. <https://doi.org/10.1007/s13205-017-0959-3>
 35. Spudich JL, Koshland DE Jr. Non-genetic individuality: chance in the single cell. *Nature* 1976;**262**:467–71. <https://doi.org/10.1038/262467a0>
 36. Checinska A, Paszczynski A, Burbank M. *Bacillus* and other spore-forming genera: variations in responses and mechanisms for survival. *Annu Rev Food Sci Technol* 2015;**6**:351–69. <https://doi.org/10.1146/annurev-food-030713-092332>
 37. Gallegos-Monterrosa R, Kovács ÁT. Phenotypic plasticity: the role of a phosphatase family rap in the genetic regulation of bacilli. *Mol Microbiol* 2023;**120**:20–31. <https://doi.org/10.1111/mmi.15060>
 38. Arnoldini M, Vizcarra IA, Peña-Miller R et al. Bistable expression of virulence genes in *salmonella* leads to the formation of an antibiotic-tolerant subpopulation. *PLoS Biol* 2014;**12**:e1001928. <https://doi.org/10.1371/journal.pbio.1001928>
 39. Philippi T, Seger J. Hedging one's evolutionary bets, revisited. *Trends Ecol Evol* 1989;**4**:41–4. [https://doi.org/10.1016/0169-5347\(89\)90138-9](https://doi.org/10.1016/0169-5347(89)90138-9)
 40. Hoskisson PA, Barona-Gómez F, Rozen DE. Phenotypic heterogeneity in *Streptomyces* colonies. *Curr Opin Microbiol* 2024;**78**:102448.
 41. Medici IF, Bartrolí L, Guaimas FF et al. The distinct cell physiology of *bradyrhizobium* at the population and cellular level. *BMC Microbiol* 2024;**24**:129. <https://doi.org/10.1186/s12866-024-03272-x>
 42. Garde S, Chodisetti PK, Reddy M. Peptidoglycan: structure, synthesis, and regulation. *EcoSal Plus* 2021;**9**. <https://doi.org/10.1128/ecosalplus.ESP-0010-2020>
 43. Amstutz J, Krol E, Verhaeghe A et al. Getting to the point: unipolar growth of *hyphomicrobiales*. *Curr Opin Microbiol* 2024;**79**:102470. <https://doi.org/10.1016/j.mib.2024.102470>
 44. Williams MA, Aliashkevich A, Krol E et al. Unipolar peptidoglycan synthesis in the *Rhizobiales* requires an essential class a penicillin-binding protein. *MBio* 2021;**12**:1–19. <https://doi.org/10.1128/mbio.02346-21>
 45. Brown PJ, de Pedro MA, Kysela DT et al. Polar growth in the alphaproteobacterial order *Rhizobiales*. *Proc Natl Acad Sci* 2012;**109**:1697–701. <https://doi.org/10.1073/pnas.1114476109>
 46. Harsh V, Maryam K, Hanna S. Non-genetic inheritance restraint of cell-to-cell variation. *elife* 2021;**10**:1–16. <https://doi.org/10.7554/eLife.64779>
 47. Smits WK, Kuipers OP, Veening J-W. Phenotypic variation in bacteria: the role of feedback regulation. *Nat Rev Microbiol* 2006;**4**:259–71. <https://doi.org/10.1038/nrmicro1381>
 48. Striednig B, Hilbi H. Bacterial quorum sensing and phenotypic heterogeneity: how the collective shapes the individual. *Trends Microbiol* 2022;**30**:379–89. <https://doi.org/10.1016/j.tim.2021.09.001>
 49. Hayat S, Faraz A, Faizan M. Root exudates: Composition and impact on plant–microbe interaction. In: Ahmad IaH, F.M. (ed.), *Biofilms in Plant and Soil Health*. Hoboken NJ USA: John Wiley & Sons Ltd. <https://doi.org/10.1002/9781119246329.ch10>